Available online at www.sciencedirect.com

SCIENCE DIRECT®

Cement and Concrete Research 35 (2005) 1804–1813

Cement and Concrete Research

Electrochemical study on inhibitors of rebar corrosion in carbonated concrete

G. Trabanelli, C. Monticelli*, V. Grassi, A. Frignani

Corrosion Study Centre "A.Dacco", Chemistry Department, University of Ferrara, L. Borsari, 46-44100 Ferrara, Italy

Received 25 January 2004; accepted 7 December 2004

Abstract

Electrochemical Impedance Spectroscopy (EIS) was used to evaluate the inhibitive action of some organic compounds towards the corrosion of a carbon steel, both in a solution simulating the pore chemistry of carbonated concrete and in carbonated concrete.

The synthetic solution (SS) has been made by bubbling pure CO_2 in a saturated $Ca(OH)_2$ solution till obtaining pH 7 and then filtering it. Concrete carbonation has been obtained by maintaining the concrete specimens in CO_2 atmosphere for 80 days, at 68% RH and room temperature.

In SS, benzoate, its amino-derivatives and dicarboxylates were able to form a long-lasting passive layer on the steel surface. Their efficiency improved with time.

In carbonated concrete the additives inducing a decrease in the concrete compressive strength were discarded. Some compounds were monitored for up to 400 days, but only two (the sodium salts of benzoic acid and, particularly, 2-amino benzoic acid) exhibited some inhibitive effect towards the rebar corrosion process.

Keywords: C. Carbonation; C. Corrosion; D. Admixture; Benzoate derivative; Electrochemical impedance spectroscopy

1. Introduction

The process of carbonation causes a pH decrease (from around 13 to around 8) in the solution present in the concrete pores. Under this condition, rebar passivity is no longer maintained and active corrosion can ensue. Therefore, as it is in the case of chloride attack [1–3], the use of proper inhibiting substances becomes particularly useful.

With this purpose, some classes of organic substances, showing good inhibiting properties towards carbon steel corrosion in near neutral, mildly saline, aqueous solutions, were tested in a solution simulating the pore chemistry of carbonated concrete (synthetic solution, SS) [4,5]. They were selected on the basis of a simple electrochemical test (polarization curves recording), carried out after only 45 min of immersion in SS. In particular, the compounds capable to prevent rebar transition from passive to active corrosion, by markedly inhibiting the anodic process on the rebar, were able to keep stable passive conditions during 30 days immersions, with inhibiting efficiencies greater than 90%. As expected, small variations in the structure of the base molecule could cause important changes in the inhibition efficiency. For instance, effective inhibitors were sodium salts of benzoic acid and its amino- or nitro-derivatives (but not the chloro-derivatives), sodium salts of saturated dicarboxylic acids or dicarboxylic poly-hydroxylated compounds (but not the monocarboxylic poly-hydroxylated ones or poly-hydroxylated substances), and sodium salts of cinnamic acid (but not the salts of chloro-cinnamic acid) [4,5].

This paper aims at concluding the previous research, by discussing and comparing Electrochemical Impedance Spectroscopy (EIS) tests carried out on steel electrodes either immersed for 20 days in SS or embedded in carbonated concrete for up to 400 days. The selection of admixtures for concrete took into consideration also the influence they exerted on the compressive strength and carbonation rate of the concrete.

* Corresponding author.
E-mail address: mtc@unife.it (C. Monticelli).

0008-8846/$ - see front matter © 2005 Elsevier Ltd. All rights reserved.
doi:10.1016/j.cemconres.2004.12.010

The EIS technique is a non-destructive technique which can highlight the inhibitor action mechanism and is often complementary to other investigation techniques such as polarization curve recording.

The EIS spectra in concrete are rather complex and always present more than one time constant.

The response of cementitious systems in the high frequency region (over 10^5 Hz) has been related by Zhongzi Xu et al. [6] to the ion concentration in the pore solutions, to the porosity and pore size distribution. According to other authors, the high frequency region of the spectra include two contributions: one due to the solid phase [7–9] and the other due to the ionic motion of free ions in the electrolyte filling the pores [10] or to imperfect electrode contacts, due to local drying and/or cracking [9].

In the middle frequency region (10^4–10 Hz range), it is possible to study the dielectric properties of a layer often formed on the steel surface and reputed to be constituted by corrosion products [11] or, according to other authors [12–14], by a protective precipitated calcium hydroxide or a lime-rich product. This film could restrain the pH drop caused by the hydrolysis of iron in pitting corrosion by a buffering effect [15]. It also limits the cathodic reaction by covering the steel surface available for oxygen reduction [16].

In the low frequency region (from a few to a few tenths of Hz), the EIS spectra are affected by the Faradaic corrosion process occurring on the embedded steel electrodes, with capacitancies in the range of tenth of microfarad per square centimeter ($\mu F\ cm^{-2}$) or higher, depending on the roughness of the surface [17]. In particular, in the case of multiple pits or generalized corrosion, as produced in carbonated mortars, the loop in the EIS spectra becomes much flatter and deformed [18].

At even lower frequencies, the impedance spectra can be affected by diffusion processes, usually attributed to oxygen diffusion, even if not enough experimental evidence has been produced so far to verify such an assumption [19]. Depending on the relative rates of the Faradaic and diffusion processes, the whole corrosion process can exhibit either activation, or a mass transfer, or a mixed control.

According to other authors, very low frequency arcs in the EIS spectra can be more confidently attributed to redox processes, of the type Fe(II) $\Leftrightarrow$Fe (III) [17,20], taking place in the steel passive layer and inducing capacitancies in the order of millifarad per square centimeter ($mF\ cm^{-2}$). They are reputed to be due to the presence of a $Fe_3O_4 \Leftrightarrow \gamma\text{-}Fe_2O_3$ equilibrium in the passive layer [20].

2. Methods

The steel specimens were obtained from AISI 1033 type steel rods (nominal composition: C=0.3%; Mn=0.96%; Ni=0.2%; Si=0.04%; Cu=0.02%; Al=0.07%; and S=0.03%; P<0.01%) normally used as concrete reinforcement.

2.1. Tests in synthetic solutions (SS)

The SS was prepared by bubbling pure CO_2 down to pH 7.0 in a filtered saturated $Ca(OH)_2$ solution. Successively, the solution was filtered again to remove precipitated calcium carbonate.

The examined substances were:

- benzoic acid (BEN) and its derivatives: 2-amino benzoic acid (2AMB) and *N*-phenyl-2-amino benzoic acid (Ph2AMB);
- dicarboxylic acids: succinic (SUC), adipic (ADI), suberic (SUB), and sebacic (SEB); and
- sodium nitrite (SN) and dicyclohexylammonium nitrite (DCHAMN), as reference compounds because they proved to be quite efficient in chloride-containing concretes [21–23] and in carbonated concretes [24]. Now their use in concrete applications is limited as they are not environmentally friendly [25].

The acids were converted into sodium salts by adding stoichiometric amounts of NaOH. The additive concentration was 0.05M. When necessary, after additive dissolution, the pH was readjusted to 7.0 by CO_2 bubbling.

The steel electrodes consisted of cylinders with an exposed surface area of 4.5 cm^2. They were ground by emery papers up to grade 600, washed with double distilled water and degreased with acetone.

2.2. Tests in concrete specimens

Concrete specimens (dimensions 25×25×3 cm) were prepared with CEM II A/L 42.5R, according to the mix design reported in Table 1. The water/cement ratio (*w*/*c*) was 0.6, with the exception of Ph2AMB-containing concrete specimens, as described in the Results and discussion section.

Each concrete specimen embedded two steel rods (diameter of 1 cm, ground down to grade 600 by emery paper) whose ends were masked with epoxy resin to leave an exposed surface area of 66 cm^2. These rods were in a central position with respect to the slab thickness and left a thin concrete cover (1 cm) which facilitated the full concrete carbonation. Three symmetrical auxiliary electrodes (stainless steel rods) and two quasi-reference electrodes (activated titanium wires) were also embedded and used for electrochemical tests. The reference electrodes were chosen in order

Table 1
Concrete mix design

Cement/kg m^{-3}	367
Water/kg m^{-3}	216
Aggregate (max. aggr. size=8 mm)/kg m^{-3}	1770
Water/cement ratio	0.6*
Additive/cement ratio/mole kg^{-1}	0.28

* 0.8 in the presence of Ph2AMB.

to be characterized by low impedance values, which should minimize their influence upon the recorded EIS spectra [17].

In the concrete admixture the organic additive amount was always kept at 0.28 mole/kg cement. The same additive/cement ratio was previously adopted in chloride-polluted mortars [1].

The uninhibited and inhibited reinforced concrete specimens were subjected to the following procedure:

step I Hardening: 3 day curing at RH>95% + 28 day aging under laboratory atmosphere conditions, at room temperature (RT);
step II Carbonation: 80 day carbonation under 68% RH, in a pure CO_2 atmosphere, RT; and
step III Exposure: partial immersion in tap water for up to 400 days.

For the evaluation of the compressive strength and carbonation rates, non reinforced cubic concrete specimens (either non containing or containing the inhibiting admixtures) were also prepared (side dimension: 10 cm) and cured for 28 day at RH>95%. For the evaluation of the carbonation rates some of these specimens underwent a step II carbonation treatment and carbonation kinetics was determined on sections of these specimens by applying the phenolphthalein method.

2.3. Electrochemical measurements

In either SS or concrete specimens, EIS spectra were collected at the corrosion potential (E_{cor}) by imposing a ±10 mV rms sinusoidal perturbation, in a frequency range 10^5–10^{-3} Hz (or 10^{-4} Hz, particularly for measurements in concrete specimens) and by collecting five measurements per decade, by a Solartron apparatus (EI 1287, FRA 1260). Before EIS spectra recording, the E_{cor} values were measured with respect to a saturated calomel electrode (SCE) (which, in concrete specimens, was connected through an external wet cotton wool pad).

On the steel rebars embedded in concrete, ohmic drop-compensated polarization curves were also recorded at the end of the 400 day exposure to the laboratory atmosphere under conditions of partial immersion in tap water. The potential was scanned from the corrosion potential to either the cathodic or the anodic direction, at a scan rate of 0.5 mV/s.

All the potential values reported in the text, unless clearly indicated, are referring to SCE.

3. Results and discussion

3.1. Tests in SS

After 1 h immersion, omitting the very high frequency arc due to the low solution conductance, EIS spectrum of steel exhibited a single capacitive semicircle in the 10^3–10^{-2} frequency range (Fig. 1), showing that the corrosion process was mainly charge-transfer controlled at short immersion times. The equivalent circuit (EC) fitting these experimental data (reported in Fig. 2a) was a resistance (R_0, the solution resistance) in series to a parallel combination of a resistance (R) and a constant phase element (CPE, which takes into account the non ideal behaviour of the system), whose impedance expression is:

$$Z_{CPE} = \frac{1}{\left[Y(j\omega)^P\right]}$$

with $0 \le p \le 1$. For $p=1$ the CPE is an ideal capacitor and then Y is equal to a capacitance; for $p=0$, CPE is a pure resistor and $Y=1/R$; and for $p=0.5$, CPE can model a diffusive process [26].

After three hours, the polarization resistance, R_p, (i.e. the difference between the real parts of the complex Faradaic impedance at zero frequency, R'_p, and the solution resistance, R_0) increased from 1.4 to 2.9 k Ω cm^2 for the likely formation (or thickening) of a corrosion product layer on the electrode and at the same time a second time constant (τ) appeared. In this case the EC fitting the experimental results included a further arm (a resistance, r, in series to a generalized finite length Warburg element, W) in parallel to the previously described R–CPE combination, as shown in Fig. 2b. The expression of W is:

$$W = R_W \cdot \frac{\tanh\left[j\omega\left(\frac{\delta^2}{D}\right)\right]^P}{\left[j\omega\left(\frac{\delta^2}{D}\right)\right]^P}$$

where δ is the effective diffusion path length, D the effective diffusion coefficient and $0 \le P \le 1$ [24]. This

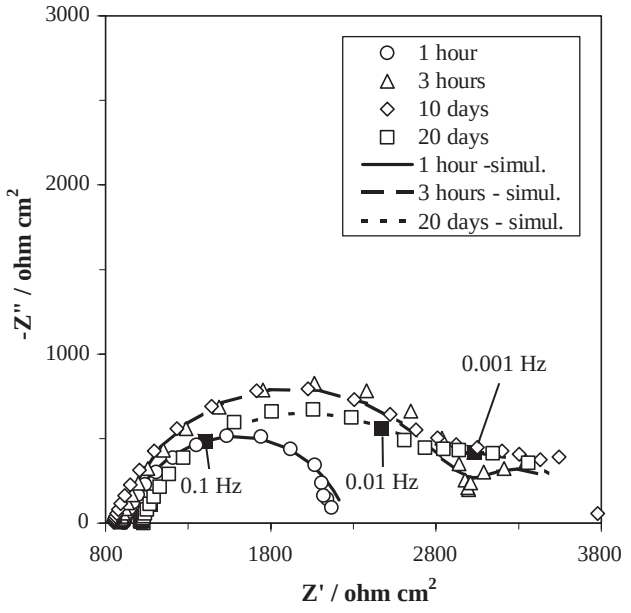

Fig. 1. Experimental and simulated EIS spectra recorded in uninhibited SS at different immersion times. The frequencies indicated refer to the 20 day spectrum.

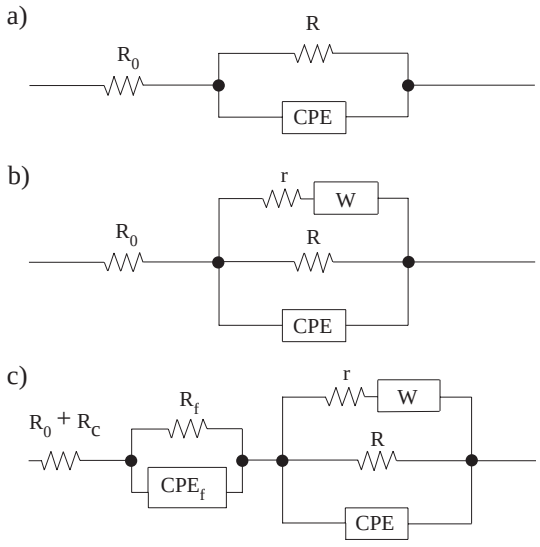

Fig. 2. Equivalent circuits used to fit the experimental spectra.

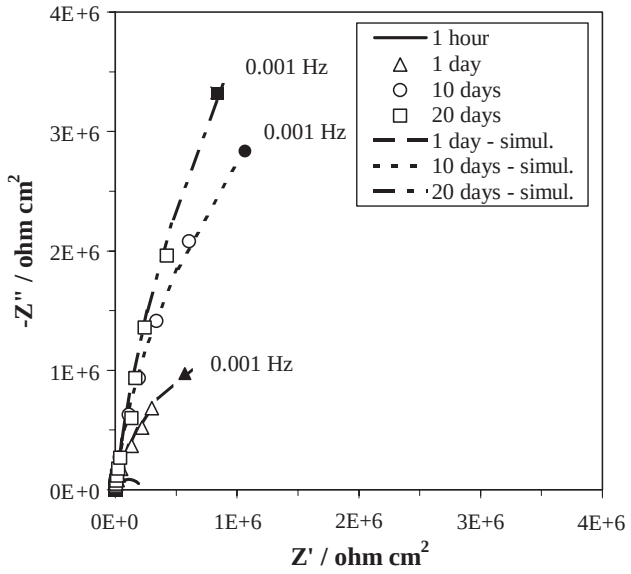

Fig. 3. Experimental and simulated EIS spectra recorded in SS in the presence of BEN, at different immersion times.

second capacitive loop (detected at frequencies lower than 10^{-2} Hz) could be attributed to a mass transfer step and indicated that, already after 3 h of immersion, the corrosion process underwent both activation and diffusion control. This loop was almost independent of time and R_p, from 3 h on, remained more or less constant and close to 3 k Ω cm^2 (Fig. 1).

Table 2 collects the parameter values which fitted the experimental data. It shows that during the test, the solution resistance (R_0) was more or less constant and close to 900 Ω cm^2. The value of R increased from 1400 (1 h immersion) up to about 5000 W cm^2 in 3 h immersion and afterwards slightly decreased till the end of the test. R was assigned to the anodic reaction, on the basis of previous results obtained in SS after 1 h immersion [4]. In fact under these conditions, the analysis of the polarization curves shows that the rate of the anodic reaction controls the rate of the corrosion process (as the anodic overvoltage is much greater than the cathodic one) and the apparent polarization resistance, R'_p (corresponding to the sum of the polarization resistance, R_p, and the solution resistance, R_0), can be obtained from the following modified Stern and Geary relation: $R'_p=b_a/i_{corr}$ (where b_a and i_{corr} correspond to the anodic Tafel slope and the corrosion current density, respectively). From Ref. [4], a R'_p value of 100×10^{-3} V/50×10^{-6} A cm^{-2}=2000 Ω cm^2 can be calculated. The EIS analysis shows that after 1 h immersion, such R'_p value should correspond to the value of $R+R_0$ (Fig. 2a). The good agreement between R'_p (2000 Ω cm^2) and $R+R_0$ (2310 Ω cm^2) values confirms that R is actually connected to the anodic process.

Over time, corrosion products accumulated on the electrode surface and oxygen diffusion rate decreased. Therefore, it is reasonable to ascribe the W element (included in the EC after 3 h immersion) to the cathodic reaction of oxygen reduction. The δ^2/D parameter value continued to increase with time, until 20 days of exposure, suggesting the formation of a massive layer of corrosion products, through which diffusion occurred. Both R_W and r fluctuated around 3000 Ω cm^2, until the end of the test.

The parameter Y was around 400 μF cm^{-2} after 1 day and shifted towards greater values during the immersion (reaching 850 μF cm^{-2}, after 10 days, and 1900 μF cm^{-2}, after 20 days), probably due to the increase in the corroded surface area. The exponent p remained close to 0.80 throughout the test.

The spectra obtained in the presence of BEN derivatives (as an example, Fig. 3 collects the Nyquist plots of the spectra recorded in BEN inhibited solution) revealed the formation of a thin, very protective layer, after only 1 h immersion. In fact, they were characterized by a capacitive

Table 2
Values of the EC parameters determined by impedance spectra

Time/h	EC parameters							
	R_0/Ω cm^2	R/Ω cm^2	Y/μF cm^{-2}	p	r/Ω cm^2	R_W/Ω cm^2	δ^2/D/s	P
1	910	1400	385	0.81	/	/	/	/
3	890	5200	260	0.84	3300	2400	210	0.5
24	880	5000	402	0.81	3200	3540	180	0.40
240	850	5000	837	0.81	3000	3500	400	0.40
480	1010	4500	1870	0.77	2900	3300	1000	0.45

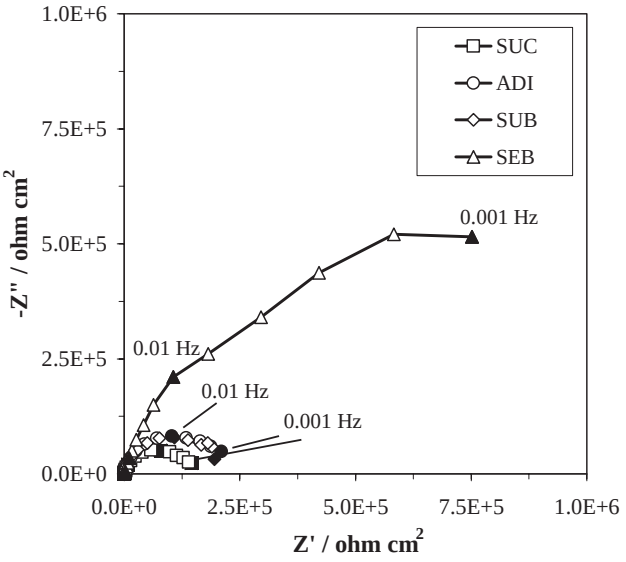

Fig. 4. Experimental EIS spectra recorded in SS in the presence of the different dicarboxylates, after 1 h immersion.

semicircle whose diameter value (around $2 \cdot 10^5$ Ω cm^2 in the case of BEN) was markedly higher than that of the blank. A noticeable increase in the resistance was found during the initial 24 h of immersion (for instance, in the case of BEN a tenfold increase was detected) and thereafter it augmented continuously, showing that the protectiveness of the layer continued to improve.

Ph2AMB was more efficient than BEN, as at the end of the test the R_p value was higher than 10^4 k Ω cm^2, whereas the presence of the –NH_2 group in the BEN molecule slightly depressed its inhibiting efficiency.

In the case of the bicarboxylic acids, the longer the aliphatic chain, the higher the polarization resistance, as shown, as an example, by the Nyquist plots recorded after 1 h immersion (Fig. 4). In the case of SEB, the most efficient additive, EIS spectrum was characterized by two not well resolved time constants.

The simple EC shown in Fig. 2a, consisting in this case of a parallel combination of a resistance (the resistance of the barrier layer-passive film, R_L) and a constant phase element (CPE_L), closely fitted the experimental data obtained in inhibited solutions (with the exception of those obtained in SEB solution). CPE_L takes into account the inhomogeneities of the metal surface and of the inhibitor layer. Table 3 collects the parameter values for most of the additives as a function of time. As can be seen, both the benzoate derivatives and dicar-

Table 3
Parameters of EC satisfying EIS spectra recorded in SS

Additive	Time/h	1	3	24	240	480
BEN	R_0/Ω cm^2	145	147	145	162	162
	R_L/Ω cm^2	$2.1 \cdot 10^5$	$3.2 \cdot 10^5$	$2.4 \cdot 10^6$	$1.4 \cdot 10^7$	$2.4 \cdot 10^7$
	Y_L/μF cm^{-2}	70	57	43	31	31
	p	0.87	0.89	0.89	0.93	0.93
2AMB	R_0/Ω cm^2	133	130	125	141	142
	R_L/Ω cm^2	$1 \cdot 10^5$	$1.6 \cdot 10^5$	$8 \cdot 10^5$	$3.7 \cdot 10^6$	$8.4 \cdot 10^6$
	Y_L/μF cm^{-2}	68	58	38	34	34
	p	0.88	0.88	0.90	0.90	0.91
Ph2AMB	R_0/Ω cm^2	/	/	/	/	/
	R_L/Ω cm^2	$1.5 \cdot 10^6$	$3.4 \cdot 10^6$	$2.2 \cdot 10^7$	$4 \cdot 10^7$	$8 \cdot 10^7$
	Y_L/μF cm^{-2}	116	84	12	15	19
	p	0.77	0.78	0.79	0.84	0.89
SUC	R_0/Ω cm^2	/	/	57	57	83
	R_L/Ω cm^2	$1.3 \cdot 10^5$	$3.2 \cdot 10^5$	$4.8 \cdot 10^6$	$8 \cdot 10^6$	$7.7 \cdot 10^6$
	Y_L/μF cm^{-2}	64	57	40	34	31
	p	0.86	0.88	0.92	0.93	0.93
ADI	R_0/Ω cm^2	82	92	83	78	94
	R_L/Ω cm^2	$2 \cdot 10^5$	$3.2 \cdot 10^5$	$4.8 \cdot 10^6$	$8 \cdot 10^6$	$7.7 \cdot 10^6$
	Y_L/μF cm^{-2}	54	50	32	32	31
	p	0.88	0.89	0.91	0.92	0.92
SUB	R_0/Ω cm^2	87	83	89	93	92
	R_L/Ω cm^2	$2 \cdot 10^5$	$4.2 \cdot 10^5$	$1.4 \cdot 10^6$	$1 \cdot 10^7$	$1.5 \cdot 10^7$
	Y_L/μF cm^{-2}	51	46	37	28	24
	p	0.89	0.90	0.88	0.93	0.92
SN	R_0/Ω cm^2	151	130	104	98	123
	R_L/Ω cm^2	$1.2 \cdot 10^5$	$3.1 \cdot 10^5$	$1.9 \cdot 10^6$	$9.9 \cdot 10^6$	$2.6 \cdot 10^7$
	Y_L/μF cm^{-2}	55	49	40	25	24
	p	0.86	0.88	0.89	0.91	0.92
DCHAMN	R_0/Ω cm^2	165	166	158	142	120
	R_L/Ω cm^2	$3.2 \cdot 10^5$	$4.8 \cdot 10^5$	$3.0 \cdot 10^6$	$1.6 \cdot 10^7$	$2.0 \cdot 10^7$
	Y_L/μF cm^{-2}	64	47	40	26	25
	p	0.76	0.86	0.88	0.91	0.91

Table 4
Slump, density and compressive strength of the different concrete mixes

Concrete type	Slump/mm	Density/kg m^{-3}	R_{compr}/MPa
Blank	50	2400	35
BEN	70	2390	28
2AMB	30	2370	30
Ph2AMB*	–	2170	6.6
SUC	60	2410	33
ADI	60	2370	25
SUB	10	2360	26
SEB	10	2360	16

* Water/cement ratio (w/c)=0.8.

boxylate compounds allowed to reach R_L values comparable or higher than those achieved in the presence of SN or DCHAMN. Such values increased during the test and often rose above 10^7 Ω cm^2. No great differences were found in the capacitance values of the passive films, which were markedly lower than that of the blank. They tended to decrease with the immersion time, suggesting that the film thickness continuously increased. At the beginning of the test, the p exponent values were close to 0.8 and increased up to about 0.9 in all the inhibited solutions, indicating the progressive healing of the film flaws.

3.2. Tests in concrete specimens

Some properties of fresh and hardened concrete mixes, obtained in the absence and in the presence of the various additives, are reported in Table 4. In the presence of Ph2AMB, it was necessary to adopt a w/c ratio higher than 0.6 (0.8), owing to the marked hydrophobic properties of the compound. Anyway, a very dry mix was obtained with this additive and low density and unacceptable compressive strength values were measured. The workability, evaluated by the slump, is low even in the presence of the two bicarboxylates with the longest aliphatic chains. All the additives negatively affected the concrete compressive strength, R_{compr}, but some of them (BEN, 2AMB, SUC) induced a limited strength decrease. In the presence of the salts of dicarboxylic acids, the longer the aliphatic chain the lower the R_{compr} decrease. In fact, ADI and SUB induced a marked reduction of the compressive strength, while, in the presence of SEB, R_{compr} was unacceptably low. Therefore, besides Ph2AMB, also SEB was discarded.

The carbonation rate was reduced by BEN, SUC, ADI, SUB, whereas SEB and, chiefly, Ph2AMB stimulated it (Fig. 5). The latter result can be ascribed to the high w/c ratio.

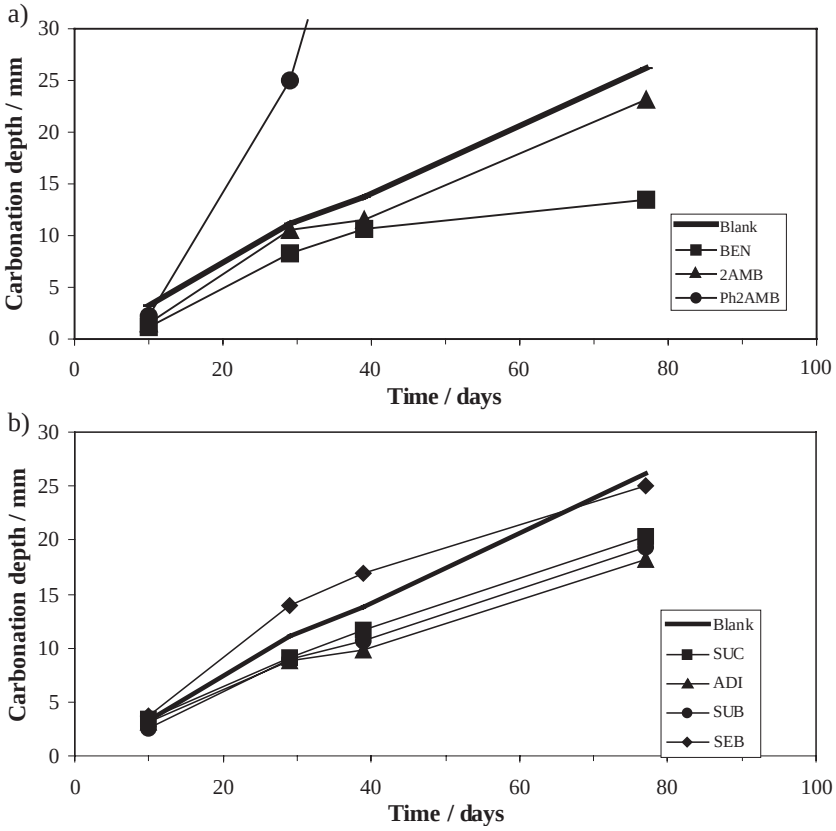

Fig. 5. Carbonation depth as a function of time in concrete mixes non containing or containing the different inhibitors: a) BEN and BEN derivatives and b) dicarboxylates.

During carbonation, E_{corr} values of the steel reinforcements settled at noble potential values, that is within −0.2 and 0 V, independently of the presence of the additives or their nature (Fig. 6). In fact, carbonation was performed in the absence of oxygen, thus the cathodic reaction and, as a consequence, the whole corrosion process was stopped.

Exposure to the laboratory atmosphere, under conditions of partial immersion, caused a quick reactivation of E_{corr} in the first week. After 37 days, these values ranged between −0.68 and −0.75 V, for the blank and bicarboxylic acid salts, while in the case of BEN and 2AMB they ranged between −0.48 and −0.43 V. After further 87 days of immersion, slightly nobler E_{corr} values were experienced by all the specimens, with the exception of BEN exhibiting a E_{corr} of about −0.58 V. At the end of the test period 2AMB kept definitely nobler E_{corr} values of the rebars, while BEN reached the values measured in the blank specimens.

3.2.1. EIS spectra

During carbonation and in carbonated moistened concrete slabs, it was not possible to study the capacitive semicircle (or semicircles [10]) related to the dielectric properties of the concrete because the high frequency limit adopted (10^5 Hz) was too low. Therefore the intercept of the high frequency part of the spectra with the real axis was taken as the sum of the solution electrolyte resistance, R_0, plus the concrete resistance, R_C, [27] and the spectra portions over that frequency limit were eliminated.

Both during and after carbonation, although lime-depleted concretes were formed, a small depressed capacitive loop was observed at intermediate frequencies (10^4–10 Hz). Under these conditions, instead of a lime or lime-rich film [12–14], a less alkaline cementitious film was probably present, whose uniformity, adherence and protectiveness towards the steel rods could be impaired by corrosion product accumulation. This capacitive loop was conveniently modelled by a parallel R_f–CPE_f circuit.

Finally at frequencies lower than 10 Hz, one or two capacitive time constants appeared, attributed to the corrosion phenomena on steel, which are substantially the same as in SS. Therefore, this last spectra portion was modelled by the same EC used for the corrosion of steel in SS.

The complete EC simulating the spectra recorded on reinforced concrete specimens during carbonation and subsequent partial immersion conditions is shown in Fig. 2c, where: R_0 and R_C correspond to the resistance of the electrolyte inside the concrete pores and to the resistance of the concrete itself, respectively; R_f and CPE_f are related to the resistive and capacitive properties of the surface film at the steel/concrete interface and CPE_f is a distributed quantity which accounts for the film inhomogeneities; and R, r, W and CPE are connected to the processes occurring at steel/concrete interface. In particular, R should correspond to the charge transfer resistance connected to the anodic partial reaction, r and W are the resistive and diffusional components induced by the oxygen reduction reaction and CPE is the double layer capacitance, exhibiting non-ideal behaviour.

The EC parameter values obtained by fitting the spectra recorded during carbonation in the blank concrete and in concretes inhibited by BEN, 2AMB and SUB (as an example of the data obtained in the presence of dicarboxylates) are reported in Table 5a.

The table shows that during the carbonation treatment the R_0+R_C parameter markedly increased because of the progressive water evaporation from pores and concrete curing. No surface film was detected in the presence of dicarboxylates, while in uninhibited concrete and in the presence of BEN and 2AMB a surface film was detected and its resistance (R_f) increased with time. In these concrete types, both the cathodic and the anodic reactions slowed down, as demonstrated by the increase with time of all the corresponding resistive parameters: R, r, and R_W. The increase in R_W was likely connected to a diminution of the oxygen content. As compared to the blank, the presence of BEN and 2AMB caused significant differences only in R_W and δ^2/D values, indicating that during carbonation the inhibitors hindered the cathodic reaction. On the contrary,

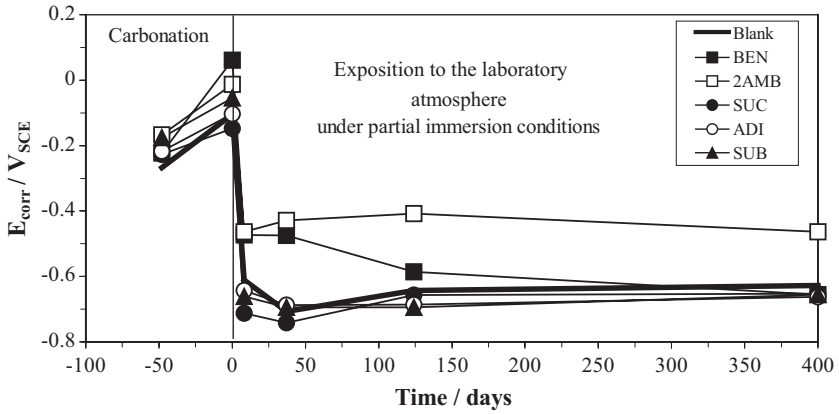

Fig. 6. Time dependence of E_{cor} of the steel rebars embedded in concrete specimens, during carbonation and during the subsequent step of partial immersion in tap water.

Table 5a
EC parameters values fitting the spectra recorded during concrete carbonation

During carbonation													
Additive	E_{corr}/V	Time/day	$R_0+R_C/10^3$ Ω cm^2	$R_f/10^3$ Ω cm^2	Y_f/μF/cm^2	p_f	$r/10^3$ Ω cm^2	$R_W/10^3$ Ω cm^2	δ^2/D/10^3 s	P	R/10^3 Ω cm^2	Y/μF/cm^2	p
Blank	−0.27	29	20	8.5	2.7	0.52	10	180	5.3	0.55	54	213	0.68
	−0.13	77	57	12	2.0	0.68	33	500	7.3	0.62	160	131	0.58
BEN	−0.22	29	12	5	/	/	10	1400	82	0.63	38	255	0.78
	+0.06	77	41	7	1.3	0.66	21	8500	78	0.56	100	65	0.61
2AMB	−0.17	29	5.6	3	/	/	8	870	31	0.57	53	270	0.87
	−0.02	77	47	8.6	2.0	0.71	7	2000	46	0.50	91	38	0.83
SUB	−0.18	29	6.2	/	/	/	/	/	/	/	130	196	0.58
	−0.06	77	21	/	/	/	/	/	/	/	45	172	0.51

the cathodic and anodic reactions were not inhibited by the presence of the bicarboxylates because the resistive parameters, r and R_W, resulted negligible and R decreased with time.

The EC parameter values fitting the most representative experimental spectra recorded during the successive partial immersion in tap water are collected in Table 5b.

As can be seen, in wet carbonated concretes, lower R_0+R_C and R_f values were detected. These lower values were due to the ingress of an electrolyte, filling or partially filling the cracks and pores present in the concrete and in the surface cementitious film, during immersion in tap water. In the presence of BEN and 2AMB, the Y_f values were one magnitude order lower than those measured in the blank specimens, indicating that these inhibitors induced a modification of the surface layer structure, which appeared more compact. Again no cementitious film was clearly detected in the presence of dicarboxylates.

In the blank specimen, the exposure to the laboratory atmosphere under partial immersion conditions markedly accelerated the cathodic process because only the loop connected to the anodic process was detected. At longer exposure times both the anodic and particularly the cathodic process progressively slowed down, as evidenced by an increase in both the resistive parameters R, r, R_W, and δ^2/D, with the latter probably connected to an increase in the length δ of the oxygen diffusion path towards the electrode.

The addition of BEN induced a marked increase in R and, particularly, R_W values, up to 124 days of exposure. Also high δ^2/D values were detected, confirming that oxygen diffusion was obstructed. However, at longer exposure times the spectra recorded in the presence of BEN became quite close to those exhibited by the blank specimen.

2AMB markedly affected the anodic process, as after 37 days of exposure R was two magnitude order higher in the 2AMB-inhibited specimen than in the blank one. The formation of a protective inhibitor passivating layer is possible, as also observed in SS. Even the cathodic process was inhibited. At longer exposure periods the 2AMB inhibiting action, although reduced, is maintained, as shown by the persistence of high R and R_W values till the end of the test. The inhibitor progressive leaching from the concrete is likely responsible of the reduced inhibition efficiency detected in BEN and 2AMB specimens at the end of the observation period. Fig. 7 shows the spectra recorded in the blank and 2AMB-inhibited specimens, after 400 days of exposure. The corresponding fitting spectra are also included.

Table 5b
EC parameters values fitting the spectra recorded on carbonated concrete, during the partial immersion in tap water

During immersion													
Additive	E_{corr}/V	Time/day	$R_0+R_C/10^3$ Ω cm^2	$R_f/10^3$ Ω cm^2	Y_f/μF/cm^2	p_f	$r/10^3$ Ω cm^2	$R_W/10^3$ Ω cm^2	δ^2/D/10^3 s	P	R/10^3 Ω cm^2	Y/μF/cm^2	p
Blank	−0.63	8	4.8	1.2	5.0	0.56	/	/	/	/	6.5	580	0.5
	−0.70	37	4.9	1.4	4.6	0.50	0.5	35	0.5	0.5	8.7	170	0.80
	−0.64	124	4.9	1.4	3.0	0.51	9.0	75	8.5	0.98	12	900	0.40
	−0.63	400	5.1	1.4	3.7	0.52	9.0	87	8.8	0.95	12	800	0.50
BEN	−0.47	8	5.7	1.3	0.23	0.78	7.1	50	1	0.67	41	342	0.40
	−0.46	37	5.4	1.4	/	/	7.5	1500	160	0.55	580	730	0.45
	−0.55	124	6.0	1.8	0.55	0.60	8.0	1500	160	0.45	100	700	0.38
	−0.65	400	4.4	1.4	0.41	0.70	9.0	110	13	0.66	22	660	0.43
2AMB	−0.44	8	9.0	7.0	0.19	0.58	15	100	2	0.58	150	160	0.31
	−0.43	37	6.0	7.0	0.64	0.50	10	300	210	0.39	1000	220	0.48
	−0.42	124	6.0	7.9	/	/	10	400	200	0.55	600	500	0.70
	−0.52	400	4.6	4.9	/	/	20	720	36	0.90	300	300	0.35
SUB	−0.66	8	2.3	/	/	/	/	/	/	/	12	900	0.50
	−0.69	37	3.6	/	/	/	/	/	/	/	8.1	640	0.52

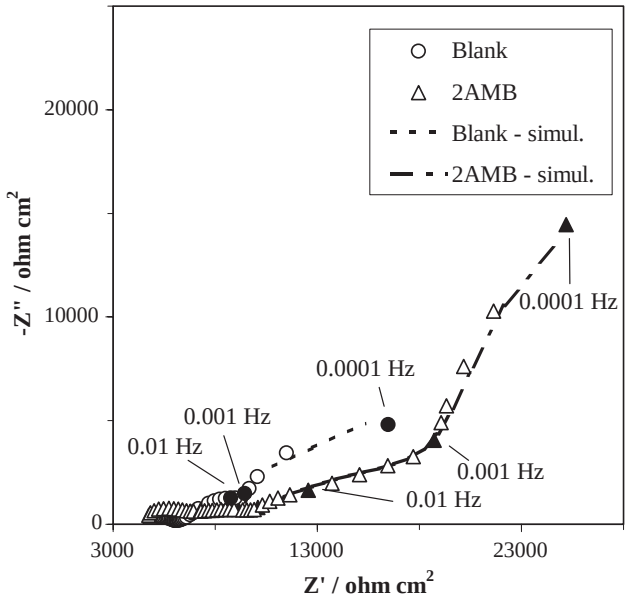

Fig. 7. Experimental and simulated EIS spectra recorded on steel rebars embedded in carbonated concrete, non containing or containing admixed 2AMB, after 400 days of partial immersion in tap water.

No dicarboxylate derivative was capable to inhibit the rebar corrosion process in carbonated concrete.

3.2.2. Polarization curves

In order to check the inhibiting efficiency of 2AMB at the end of the exposure period and to confirm the correctness of EIS spectra interpretation, ohmic drop-compensated polarization curves were recorded on the steel rebars embedded in carbonated concrete, either non containing or containing BEN and 2AMB (Fig. 8; the potentials are in this case referred to the internal reference electrode).

The analysis of the curves confirmed that at the end of the immersion period no inhibiting efficiency was obtained in the BEN-containing specimen, as the polarization curves almost overlapped those recorded in the blank specimen. On the contrary, in the presence of 2AMB, a marked shift of the anodic curve towards lower current densities suggested that this additive is mainly an anodic inhibitor. As 2AMB also induced an increase in the parallel resistance R of the EC reported in Fig. 2c, these findings confirmed that R was connected to the charge transfer resistance of the anodic process. The analysis of the polarization curves allowed the evaluation of the inhibiting efficiency of 2AMB towards the rebar corrosion process that resulted to be around 60%.

4. Conclusions

The following conclusions can be drawn:

- In SS, benzoate, its amino-derivatives and dicarboxylates were able to form a long-lasting passive layer on the steel surface. Their efficiency improved with time.
- Ph2AMB and SEB used as concrete admixtures afforded unacceptably low compressive strength values. They also stimulated the concrete carbonation rate, while BEN, SUC, ADI or SUB addition reduced it.
- Among the additives tested as admixed inhibitors in carbonated concrete, only BEN and 2AMB exhibited some inhibitive effect towards the rebar corrosion process. However, in BEN-containing concrete specimens no inhibitive action was maintained till 400 days of exposure, while in the presence of 2AMB inhibiting efficiencies around 60% were still measured at the end of the test. The inhibitor leakage is reputed responsible of the decrease with time in the inhibiting efficiency of both additives.

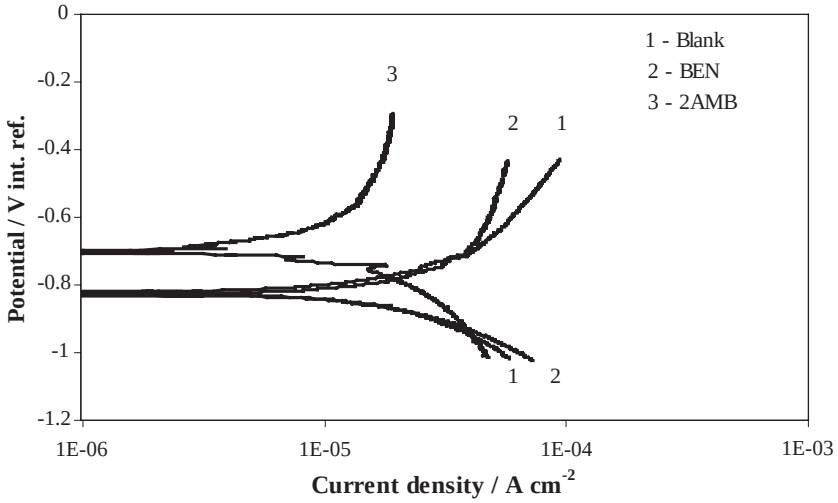

Fig. 8. IR drop-compensated polarization curves, recorded on steel rebars embedded in carbonated concrete, non containing or containing admixed inhibitors, after 400 days of partial immersion in tap water.

– 2AMB mainly hindered the anodic process of steel oxidation.

Acknowledgements

The authors wish to thank Dr. Ing. M. Ormellese of the Politecnico di Milano for the concrete specimen preparation and for the slump, density and compressive strength measurements on the different concrete mixes.

References

[1] C. Monticelli, A. Frignani, G. Trabanelli, G. Brunoro, A study on the inhibiting efficiency of a glycerophosphate–nitrite admixture against steel corrosion in mortars, in: N.S. Ferrara, V. Sez (Eds.), Proc. 8th European symposium on corrosion inhibitors, Ferrara, 18–22 Sept., 1995, Ann. Univ., vol. 1, 1995, pp. 609–620 Suppl. No. 10.

[2] C. Monticelli, A. Frignani, G. Trabanelli, A study on corrosion inhibitors for concrete application, Cem. Concr. Res. 30 (2000) 635–643.

[3] C. Monticelli, A. Frignani, G. Trabanelli, Corrosion inhibition of steel in chloride-containing alkaline solutions, J. Appl. Electrochem. 32 (2002) 527–535.

[4] C. Monticelli, A. Frignani, G. Brunoro, G. Trabanelli, Corrosion inhibitors for application in carbonated mortars, in: N.S. Ferrara, V. Sez (Eds.), Proc. 9th European symposium on corrosion inhibitors, Ferrara, 4–8 Sept., Ann. Univ., vol. 1, 2000, pp. 277–288 Suppl. No.11.

[5] G. Trabanelli, C. Monticelli, V. Grassi, A. Frignani, F. Zucchi, Inibitori di corrosione dell'acciaio per applicazione nel calcestruzzo carbonatato, Proc. Giornate Nazionali sulla Corrosione e Protezione, 5th ed., AIM, Bergamo, 2002 (21–22 May), pp. 377–385.

[6] Zhongzi Xu, Ping Gu, Ping Xie, J.J. Beaudoin, Application of a.c. impedance techniques in studies of porous cementitious materials—II. Relationship between ACIS behaviour and the porous microstructure, Cem. Concr. Res. 23 (1993) 853–862.

[7] M. Keddam, H. Takenouti, X.R. Nóvoa, C. Andrade, C. Alonso, Impedance measurements on cement paste, Cem. Concr. Res. 27 (1997) 1191–1201.

[8] C. Andrade, V.M. Blanco, A. Collazo, M. Keddam, X.R. Nóvoa, H. Takenouti, Cement paste hardening process studied by impedance spectroscopy, Electrochim. Acta 44 (1999) 4313–4318.

[9] S.J. Ford, J.D. Shane, T.O. Mason, Assignment of features in impedance spectra of the cement–paste/steel system, Cem. Concr. Res. 28 (1998) 1737–1751.

[10] C. Alonso, C. Andrade, M. Keddam, X.R. Nóvoa, H. Takenouti, Study of the dielectric characteristics of cement paste, Mat. Sci. Forum 289–292 (1998) 15–28.

[11] D.G. John, P.C. Searson, J.L. Dawson, Use of AC impedance technique in studies on steel in concrete in immersed conditions, Br. Corros. J. 16 (1981) 102–106.

[12] F. Wenger, J. Galland, L. Lemoine, Application of electrochemical impedance measurements to the monitoring of corrosion of reinforced concrete structures in marine environment, Proc. Eurocorr '87, Karlsruhe, April 6–10, DECHEMA, Frankfurt am Mein, 1987, pp. 625–631.

[13] A. Carnot, I. Frateur, P. Marcus, B. Tribollet, Corrosion mechanisms of steel concrete moulds in the presence of a demoulding agent, J. Appl. Electrochem. 32 (2002) 865–869.

[14] W. Morris, A. Vico, M. Vázquez, The performance of a migrating corrosion inhibitor suitable for reinforced concrete, J. Appl. Electrochem. 33 (2003) 1183–1189.

[15] P. Lambert, C.L. Page, P.R.W. Vassie, Investigation of reinforcement corrosion: 2. Electrochemical monitoring of steel in chloride-contaminated concrete, Mat. Struct. 24 (1991) 351.

[16] C.L. Page, Mechanism of corrosion protection in reinforced concrete marine structures, Nature 258 (11) (1975) 514–515.

[17] C. Andrade, L. Soler, X.R. Nóvoa, Advances in electrochemical impedance measurements in reinforced concrete, Mat. Sci. Forum 192–194 (1995) 843–856.

[18] C. Andrade, C. Alonso, J.A. Gonzalez, Mat. Sci. Forum 44–45 (1988) 329.

[19] M.A. Pech-Canul, P. Castro, Corrosion measurements of steel reinforcement in concrete exposed to a tropical marine atmosphere, Cem. Concr. Res. 32 (2002) 491–498.

[20] C. Andrade, P. Merino, X.R. Nóvoa, M.C. Pérez, L. Soler, Passivation in reinforcing steel in concrete, Mat. Sci. Forum 192–194 (1995) 891–898.

[21] N.S. Berke, A. Rosenberg, Technical review of calcium nitrite corrosion inhibitor in concrete, concrete bridge design and maintenance: steel corrosion in concrete, Transp. Res. Rec. 1211 (1989) 18.

[22] N.S. Berke, A. Rosenberg, Calcium nitrite corrosion inhibitor in concrete, in: E. Vazquez (Ed.), Admixtures Concr. Proc. Int. Symp., Chapman and Hall, London, 1990, p. 251.

[23] A. Phanasgaaonkar, M. Forsyth, B. Cherry, Organic corrosion inhibitors to mitigate corrosion of steel rebar in reinforced concrete, Proc. 13th Int. Corros. Congr., Melbourne, Australia, Paper No. 178, 1996.

[24] C. Alonso, M. Acha, C. Andrade, Inhibiting effects of nitrites on the corrosion of rebars embedded in carbonated concrete, in: E. Vazquez (Ed.), Admixtures Concr. Proc. Int. Symp., Chapman and Hall, London, 1990, p. 219.

[25] B. Elsener, Corrosion inhibitors for steel in concrete—state of the art report, European Federation of Corrosion publications, no. 35, Maney Publishing, London, 2001.

[26] Electrochemical impedance sofware Zplot for Windows®, 1998.

[27] W.J. McCarter, R. Brousseau, The a.c. response of hardened cement paste, Cem. Concr. Res. 20 (1990) 891–900.